

Identifying the $\nu = \frac{5}{2}$ topological order through charge transport measurements

Misha Yutushui, Ady Stern, and David F. Mross

Department of Condensed Matter Physics, Weizmann Institute of Science, Rehovot, 76100, Israel

(Dated: May 15, 2022)

We propose an experiment to identify the topological order of the $\nu = \frac{5}{2}$ state through a measurement of the electric conductance of a mesoscopic device. Our setup is based on interfacing $\nu = 2$, $\frac{5}{2}$ and 3 in the same device. Its conductance can unambiguously establish or rule out the particle-hole symmetric Pfaffian topological order, which is supported by recent thermal measurements. Additionally, it distinguishes between the Moore-Read and Anti-Pfaffian topological orders, which are favored by numerical calculations.

Introduction. Fractional quantum Hall (FQH) states^{1–4} comprise many fascinating aspects of quantum many-body physics in an experimentally available platform. These features include topological order, which is reflected in fractional quantum numbers and statistics, and topologically protected edge states.⁵ The latter lead to robust experimental signatures such as a perfectly quantized electronic Hall conductance. A special group among the plethora of fractional quantum Hall states are those that exhibit highly-prized non-Abelian statistics.^{6–9} The strongest numerical evidences of such a phase arise at the filling factor $\nu = \frac{5}{2}$.^{10–17} The nature of this phase remains hotly debated; the leading candidates based on numerical simulations are the celebrated Moore-Read Pfaffian,⁸ and its particle-hole conjugate, known as anti-Pfaffian.^{18,19}

The experimental distinction between different $\nu = \frac{5}{2}$ states is challenging due to the similarity of their edge structures: they feature the same charged modes and differ only in the number of Majorana modes. The parity of that number may be observed by interference measurements,^{20–22} but a full identification of the topological order requires measurements of the thermal Hall conductance. Ref. 23 measured the two-terminal thermal conductance to be $\kappa \approx \frac{5}{2}$ (in units of $\pi^2 k_B^2 T/3h$; where k_B, h are the Boltzmann and Planck constants). By contrast, the quantized values for Pfaffian and anti-Pfaffian are $\frac{7}{2}$ and $\frac{3}{2}$. The measured value matches theoretical expectations for the PH-Pfaffian phase,²⁴ which is PH invariant²⁵ but faces theoretical challenges:^{26,27} It has never been observed numerically, and its trial states become critical upon projection into a single Landau level.^{28–31} Subsequent theoretical works argued that incomplete anti-Pfaffian edge equilibration might also realize the measured value.^{32–37}

More recently, thermal noise measurements Ref. 38 have further strengthened the case for PH-Pfaffian. The latter experiments interfaced $\nu = \frac{5}{2}$ states with $\nu = 3$ to realize the PH conjugate of the standard edge between $\nu = \frac{5}{2}$ and $\nu = 2$. Observing the noise in both cases suggests that both ‘direct’ and particle-hole conjugate edges contain counter-propagating modes, which is the case only for PH-Pfaffian.

In this work, we show that devices that simultaneously contain interfaces of $\nu = \frac{5}{2}$ with $\nu = 2$ and $\nu = 3$ can

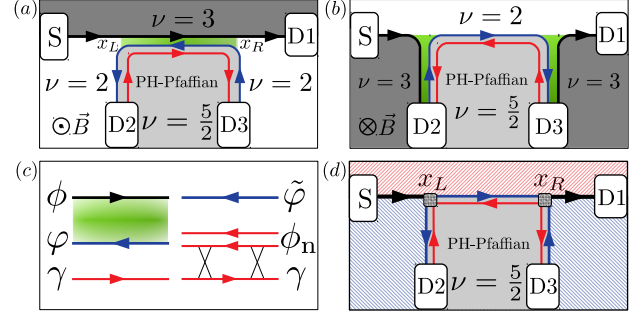


Figure 1. Our setup exemplified for the PH-Pfaffian topological order. The $\nu = \frac{5}{2}$ region is interfaced with $\nu = 2$ and $\nu = 3$. The positions of the integer states are interchanged between (a) and (b). Tunneling renormalizes the density-density interactions between electron (**black**) and semion (**blue**) modes to a fixed point with decoupled charge and neutral (**red**) modes (c). The neutral mode is partially compensated by the Majorana mode, leading to the same minimal edge structure in both cases [see (d)].

provide critical information about the topological order at $\nu = \frac{5}{2}$. Specifically, we find that electric conductances in such devices take different universal values depending on whether the edges with $\nu = 2$ or with $\nu = 3$ are chiral, i.e., carry only co-propagating modes. The former includes the Moore-Read state, the latter the anti-Pfaffian. Among the candidate topological orders, only PH-Pfaffian features achiral edges with both $\nu = 2, 3$ and can therefore be identified uniquely.

In the setup of Fig. 1, a single electron mode emanates from the source S and enters the drain D1. Consequently, the conductance G must lie between zero and one in units of e^2/h . If it were solely determined by the bulk filling factors, the value $G = \frac{1}{2}$ would arise. We instead find that, at zero temperature, the conductance can be either $G = \frac{1}{2}$ or $G = 1$ and is dictated by the nature of the $\nu = \frac{5}{2}$ state. For the filling factors as in Fig. 1(a), we predict complete transmission $G = 1$ for the Moore-Read but $G = \frac{1}{2}$ for PH-Pfaffian and anti-Pfaffian; in the PH-conjugate setup of Fig. 1(b), we expect full transmission for anti-Pfaffian and $G = \frac{1}{2}$ for both Moore-Read and PH-Pfaffian. Thus, two charge measurements on the same device can distinguish between the three candidates.

Quantum Hall states in the half-filled first excited Landau level. The different electronic Hall conductances of the $\nu = \frac{5}{2}$ and $\nu = 2$ states require a specific chiral charge mode at their interface. In addition, there are a number n_M of neutral chiral Majorana modes γ_i that depend on the specific topological phase. The edge Lagrangian density reads $\mathcal{L}_{\text{edge}} = \mathcal{L}_0 + \delta\mathcal{L}$ with

$$\mathcal{L}_0 = \frac{\text{sgn}(v)}{2\pi} \partial_x \varphi [\partial_t - v \partial_x] \varphi + i \sum_{l=1}^{n_M} \gamma_l [\partial_t - v_l \partial_x] \gamma_l, \quad (1)$$

where $s \propto e^{i\varphi}$ creates a charge- $e/2$ semion. For the Moore-Read state $n_M = 1$, and the charge- and neutral-mode velocities v, v_1 have equal signs. Their signs are opposite for both PH-Pfaffian, which has $n_M = 1$, and anti-Pfaffian with $n_M = 3$. The edge theory \mathcal{L}_0 admits interactions between charge and neutral modes, e.g., $\delta\mathcal{L}_1 \propto \partial_x \varphi \gamma_i \gamma_j$ or $\delta\mathcal{L}_2 \propto \partial_x \varphi \gamma_j \partial_x \gamma_j$. The scaling dimensions $[\gamma] = \frac{1}{2}$, $[s] = \frac{1}{4}$, and $[\varphi] = 0$ imply that $\delta\mathcal{L}_1$ is marginal and $\delta\mathcal{L}_2$ is irrelevant in the RG sense. The former may change the edge conductance, while the latter does not affect macroscopic observables.³⁹

For the analysis of our proposed device setups, we also need the field theory of the hole-conjugate edge. It is obtained by adding to $\mathcal{L}_{\text{edge}}$ a chiral mode of electrons $\psi^\dagger \sim e^{i\phi}$ described by

$$\mathcal{L}_e = \frac{\text{sgn}(v_e)}{4\pi} \partial_x \phi [\partial_t - v_e \partial_x] \phi, \quad (2)$$

with chirality opposite to the semion mode φ . The two edge theories $\mathcal{L}_e, \mathcal{L}_{\text{edge}}$ couple via density-density interactions $\mathcal{L}_{\text{int}} = 2h \partial_x \phi \partial_x \varphi$ and electron tunneling $\mathcal{L}_{\text{tun}} \propto i \sum_j \lambda_j \gamma_j \psi^\dagger s^2$. The amplitudes λ_j generically contain x -dependent phase factors that cause destructive interference. Impurities, which result in randomly varying $\lambda_j(x)$, destroy this interference and facilitate tunneling between different edge modes.^{40–45} Random tunneling is relevant when the scaling dimension of $\gamma_j \psi^\dagger s^2$ is smaller than $3/2$. For $h = 0$, we have $[\gamma_j \psi^\dagger s^2]_{h=0} = 2$ and tunneling is irrelevant; it becomes relevant for sufficiently strong interactions $h > h_c \equiv \frac{6-\sqrt{6}}{12}(v + v_e)$.^{18,19}

To analyze the latter case, we introduce a new semion $\tilde{s} = \psi s^\dagger$ and a new neutral fermion $\psi_n = \psi^\dagger s^2$. These modes counter-propagate, with the chirality of \tilde{s} opposite to that of s . The Gaussian terms in the action of the composite edge correspond to kinetic terms for ψ_n, \tilde{s} and a coupling analogous to \mathcal{L}_{int} , which vanishes when $h = h_* \equiv \frac{2}{3}(v + v_e)$.^{18,19} The tunneling for non-zero n_M takes the form

$$\mathcal{L}_{\text{tun}} = i \sum_{l=1}^{n_M} \lambda_l(x) \gamma_l \psi_n + \lambda_l^*(x) \gamma_l \psi_n^\dagger. \quad (3)$$

When ψ_n , which comprises two Majoranas, and γ_l have opposite chirality, pairs of counter-propagating Majoranas can ‘compensate’ each other: They become localized at a scale ξ and do not affect the physics at longer wavelengths.⁴⁶ The remaining $|2 - n_M|$ (for opposite signs

of v, v_1) or $2 + n_M$ (for equal signs) Majoranas enjoy topological protection. They may interact with the charge mode $\tilde{\varphi}$ through terms such as $\delta\mathcal{L}_{1,2}$. However, such couplings become irrelevant at a random edge.^{18,19} Consequently, charge and neutral sectors decouple in all cases pertinent here.

PH-Pfaffian. Equipped with this general framework, we now focus on the case PH-Pfaffian in the setup of Fig. 1. This topological order is unique in having the same minimal edge structures when interfaced with $\nu = 2$ and $\nu = 3$ [as in fig. 1(d)], up to a global reversal of chirality. This property follows from Eq. (3), which localizes a pair of counter-propagating Majoranas and leaves behind an unpaired one propagating oppositely to \tilde{s} .

In Fig. 1(a), the PH-Pfaffian island is immersed in a $\nu = 2$ region adjacent to a $\nu = 3$ region. We consider the case where D1, D2, D3 are all grounded, while the source is at a potential V . The conductance measurement is then a scattering experiment, with the incoming state being an electron emanating from the source. Outgoing states must carry the electron charge either as an electron going to D1 or two semions going to D2. In the latter case, there must also be a Majorana fermion going into D3 to conserve fermion parity. We use the currents at S, D1, D2, D3 as boundary conditions for the segment between $x_{R/L}$ to calculate the conductance. The current emanating from S propagates unimpeded to x_L and is carried by electrons. As such, it is $I_e^S = \partial_t \phi(x_L)/2\pi$. Similarly, the current that enters D1 is $I_e^{D1} = \partial_t \phi(x_R)/2\pi$. The currents from D3 and into D2 are carried by semions and are given by $I_{\text{qp}}^{D2, D3} = -\partial_t \varphi(x_{L,R})/2\pi$.

In the middle region, charge mode $\tilde{s}^\dagger \propto e^{i\tilde{\varphi}}$ and neutral mode $\psi_n \propto e^{i\phi_n}$ decouple. The corresponding charge current is $I_c = I_e - I_{\text{qp}}$, and the neutral current is $I_n = I_e - 2I_{\text{qp}}$. The boundary conditions are thus

$$\begin{aligned} I_c(x_L) &= I_e^S - I_{\text{qp}}^{D2}, & I_n(x_L) &= I_e^S - 2I_{\text{qp}}^{D2}, \\ I_c(x_R) &= I_e^{D1} - I_{\text{qp}}^{D3}, & I_n(x_R) &= I_e^{D1} - 2I_{\text{qp}}^{D3}. \end{aligned} \quad (4)$$

Charge conservation implies $I_c(x_R) = I_c(x_L)$, but the neutral current is sensitive to interactions at the interface. In the absence of the tunneling term \mathcal{L}_{tun} , $I_n(x_L) = I_n(x_R)$ and any current emanating from S flows into D1. By contrast, when tunneling localizes one of the Majorana modes, then $I_n(x_L)$ vanishes exponentially with $|x_L - x_R|/\xi$. A neutral fermion at x_R has equal probabilities for arriving as a hole or as a particle at x_L .⁴⁷ Consequently, the source current splits equally between D1 and D2, and the conductance is $G = \frac{1}{2}$.^{48–50}

One may worry that the conductance might be affected by local processes that couple the neutral and charge modes and lead to $I_n(x_L) \neq 0$. The most dangerous coupling is an interaction between charge and neutral modes of the form $\partial_x \tilde{\varphi} e^{2i\phi_n} + H.c.$ It is, however, irrelevant and does not affect the conductance at low voltages.

The relation between the minimal edge structures of

the $\nu = 2, 3$ interfaced with the PH-Pfaffian state implies that the same result holds for the PH-conjugate setup of Fig. 1(b) when inter-edge tunneling is strong [see Fig. 1(d)]. It is instructive to analyze this setup starting from the limit where the different edge modes in Fig. 1(b) are decoupled. Then, all the current that emanates from S enters D2 and $G = 0$. When the edges are coupled by density-density interactions only, the eigenmodes between $x_{L,R}$ and D2,D3 are h -dependent linear combinations of the counter-propagating electron and semion modes. As shown in the appendix A, there is a flow of current from S to D1, with an h -dependent non-universal conductance. For the $h = h_*$, the eigenmodes are the charge and neutral modes, and $G = 1/2$. Strong tunneling localizes one of two Majorana fermions comprising ψ_n . It thereby prohibits marginal couplings between charge and neutral sectors and enforces a universal conductance $G = 1/2$.

Moore-Read and anti-Pfaffian. We now turn to the case of a Moore-Read state in the configuration of Fig. 2(a). Its interface with $\nu = 3$ is described by Eqs. (1,2,3). Crucially, the neutral fermion ψ_n and γ co-propagate and cannot become localized by Eq. (3). Instead, the primary effect of this term is to renormalize h to h_* , thus decoupling charge and neutral modes^{18,19}. We again compute the conductance using Eq. (4). Without tunneling, $I_n(x_L) = I_n(x_R)$ and $G = 1$, as in the case of PH-Pfaffian. When tunneling is allowed, a neutral fermion at x_R has a non-zero bare amplitude for arriving at x_L as a hole. At voltages higher than a scale $\propto |x_L - x_R|^{-1}$ this leads to a non-universal differential conductance. At low voltages, the bare amplitude is renormalized. Low energy modes experience the interface region as effectively a point-like. To identify possible fixed points and find the flow near them, we replace the interface with boundary conditions for the lead variables at $x_{R,L}$. The trivial fixed point is without tunneling and $G = 1$ is encoded by $\psi_n(x_L) = \psi_n(x_R)$.^{45,48-50} The opposite limit corresponds to $\psi_n(x_L) = \psi_n^\dagger(x_R)$. Here, Eq. (4) with $I_n(x_L) = -I_n(x_R)$ yields $G = \frac{1}{3}$. Analogous fixed points were found in the context of $\nu = 2/3$ in Ref. 45. The stability of these two fixed points is determined by the relevance of the most prominent local perturbation, the tunneling term \mathcal{L}_{tun} , now acting at one point $x_L \approx x_R$. At the trivial fixed point, the neutral fermion is expressible in terms of incoming modes via $\psi_n = s^2(x_R)\psi^\dagger(x_L)$. As such, its scaling dimension is $[\psi_n] = 3/2$, while $[\gamma] = 1/2$ as before. Consequently, this perturbation is irrelevant, and the trivial fixed point with $G = 1$ is attractive. At the non-trivial fixed point, the neutral fermion satisfies $\psi_n^{\dagger 3} = s^2(x_R)\psi^\dagger(x_L)$ and thus $[\psi_n] = 1/6$. Here, the perturbation is relevant, and the fixed point is repulsive (see appendix B). Consequently, the conductance is generically determined by the trivial fixed point with $G = 1$.

The analysis of the Moore-Read state in the geometry of Fig. 2(b) mirrors that of the PH-Pfaffian. Without inter-edge coupling $G = 0$, while density-density

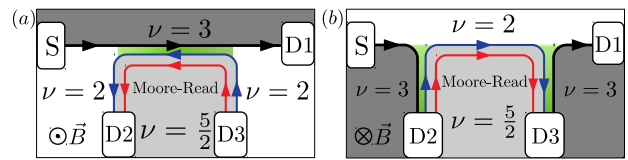


Figure 2. The same setup as in Fig. 1 for the Moore-Read topological order. (a) The tunneling between electron mode and Moore-Read edge is irrelevant, leading to a total transmission in the limit of zero temperature, $G = 1$. (b) Tunneling drives the edge connected to D2,D3 to a fixed point with decoupled charge and neutral modes and $G = \frac{1}{2}$.

interactions without tunneling lead to a non-universal h -dependent conductance. Strong tunneling results in $h = h_*$,^{18,19} for which $G = 1/2$. Local perturbations near x_L are irrelevant, as for the PH-Pfaffian, and do not modify the conductance at low voltage.

The properties of the anti-Pfaffian phase follow immediately from a global PH-conjugation $\nu = 3 \leftrightarrow \nu = 2$. Consequently, $G = \frac{1}{2}$ in the geometry of Fig. 2(a) and $G = 1$ for Fig. 2(b).

Island geometry. As an alternative to the geometries of Figs. 1, 2 one may consider a $\nu = \frac{5}{2}$ island of size $L_x \times L_y$ ‘floating’ on a $\nu = 2, 3$ background, see Fig. 3 and Refs. 45 and 51. Here, the source and the drain are connected only to integer modes. For sufficiently low energies, the fractional island acts as a local scatterer with transmission $\mathcal{T}(\omega)$ and reflection $\mathcal{R}(\omega)$ probabilities that depend on the energy of the incident electron. When the island is large compared to microscopic length scales, the bare probability amplitudes \mathcal{R}, \mathcal{T} are renormalized. On general grounds, we expect the existence of trivial fixed points with either full transmission $\mathcal{T} = 1$ [Fig. 3(a)] or full reflection $\mathcal{R} = 1$ [Fig. 3(b)]. Since the leads contain only integer modes, they do not cause renormalization, and the island’s dimensions cut off the flow.

When examining the stability of both fixed points, we find that for the Moore-Read and anti-Pfaffian states, one is stable, and the other is unstable. By contrast, both fixed points are unstable for the PH-Pfaffian, necessitating the existence of an additional, non-trivial fixed point. The qualitative behavior near the trivial fixed points is straightforward: When tunneling along the horizontal path is weak, the island exhibits discrete energy levels with splitting $\Delta E \propto \frac{1}{L_x + L_y}$. Transmission past the island is nearly perfect unless the energy of the scattering electron matches one of these levels. The conductance exhibits sharp dips at those energies, which broaden as the integer modes hybridize more strongly with the island. In the opposite limit, there is a near-perfect reflection, and the conductance is low apart from sharp resonance peaks. For a particular topological phase of the island, the renormalization of tunneling determines which limit is realized.

Consider first the case of a Moore-Read island. Near the $\mathcal{T} = 1$ fixed point, [Fig. 3(a)], \mathcal{L}_{tun} contains only

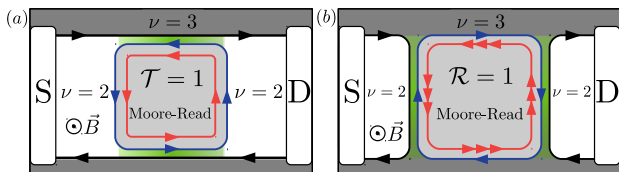


Figure 3. The two-terminal setup with the $\nu = \frac{5}{2}$ island in the Moore-Read phase, embedded in a $\nu = 2, 3$ environment. (a) The fully transmitting $\mathcal{T} = 1$ fixed point is stable in the limit $L_y \gg L_x$. (b) The fully reflecting $\mathcal{R} = 1$ fixed point is unstable in the limit $L_y \gtrsim \xi$.

co-propagating modes. The horizontal edge is characterized by decoupled charge and neutral modes. This segment is governed by a stable fixed point where no charge transfers between the electron and semion modes. For $L_x \ll L_y$, renormalization due to the vertical edges is effective, and the resonances *sharpen* at low incident energies. The transmission is thus close to unity at generic energies. When $L_y \ll L_x$, renormalization is inefficient, and deviations from complete transmission are significant. The $\mathcal{T} = 1$ fixed point is thus (marginally) stable in the Moore-Read case.

In contrast, at the $\mathcal{R} = 1$ fixed point, [Fig. 3(b)] the island decouples from the $\nu = 2$ region. Tunneling described by Eq. (3) is strongly relevant, and two pairs of Majorana modes localize at the scale ξ . Thus, the decoupling becomes unstable if $L_y \gtrsim \xi$ and the transmission resonances broaden as the energy of the incident electron decreases. For anti-Pfaffian, the two cases are reversed, and $\mathcal{R} = 1$ is marginally stable.

For the PH-Pfaffian case, we again start by perturbing around the fixed point $\mathcal{R} = 1$. Similar to the Moore-Read case, tunneling is strongly relevant. It leads to localization of a single pair of Majorana modes at the length $\xi \ll L_y$, which destroys the fully reflecting fixed point. The same reasoning also holds near $\mathcal{T} = 1$, i.e., both trivial fixed points are unstable. Therefore, when $L_x, L_y \gg \xi$, the transport must be governed by an intermediate, stable fixed point. Since the details of the island drop out in this limit, we expect this fixed point to exhibit the universal conductance $G = 1/2$ and no resonances.

Non-zero temperatures. Up to this point, our analysis assumed zero temperature $T = 0$, where all transport is fully coherent. At very low temperatures, the results still hold with power-law corrections governed by the leading irrelevant operators at the respective fixed points.

When T is large enough that the dephasing length is much shorter than the length $|x_R - x_L|$ of the interface (while still much lower than the bulk gap for delocalized excitations), the system behaves like a network of classical resistors. When dephasing is strong enough to

establish a local chemical potential at x_L [see Fig. 1], the current arriving from the source splits equally between the arms leading to D1, D2, resulting in $G = 1/2$ for all candidate states, just as the low-temperature result for the PH-Pfaffian (see also Ref. 52, which studied a related geometry). In principle, the temperature dependence of G provides a way to distinguish between the coherent and incoherent origins of $G = 1/2$. While in the former case, deviations from $1/2$ increase with temperature, in the latter, they decrease. Alternatively, coherence may be probed by incorporating an interference loop for the integer states.

Discussion. We have proposed two experimental setups where coherent charge-transport measurements can distinguish between three classes of $\nu = \frac{5}{2}$ states. (i) Those whose interfaces with $\nu = 2$ are chiral, e.g., Moore-Read. (ii) States that exhibit chiral interface with $\nu = 3$, e.g., anti-Pfaffian. (iii) The PH-Pfaffian whose interfaces with both $\nu = 2, 3$ are non-chiral. Within each setup, two charge measurements can uniquely identify the class of the state, see Tab. I. Both setups require a specific hierarchy of length scales: The localization length ξ is to be the shortest scale to guarantee that each edge state is reduced to its topologically required minimum. The thermal length $L_T \propto 1/T$ must be the longest scale to ensure coherent transport. Additionally, the island geometry requires measurements for both limits of the aspect ratios $L_x \gg L_y$ and $L_y \gg L_x$, or for two configurations related to one another by $\nu = 2 \leftrightarrow \nu = 3$.

Finally, the same information about the topological order may be obtained from a setup where the $\nu = 2$ state is substituted by $\nu = 0$. The additional integer edge modes add 2 units to the conductance in the setup referred to in the second and fourth columns of Table (I). In the same way, one can modify the system by increasing the $\nu = 3$ filling factor to a larger integer.

Table I. The conductance between the source S and the drain D1 for two different sets of filling factors, with non-univ. standing for ‘non-universal’ conductance bounded between 0 and 1.⁵¹ The last column corresponds to the setup of Fig. 3 with interchanged $\nu = 2$ and $\nu = 3$ states.

	Fig. 2(a)	Fig. 2(b)	Fig. 3	Fig. 3 ($2 \leftrightarrow 3$)
Moore-Read	1	1/2	1	non-univ.
PH-Pfaffian	1/2	1/2	1/2	1/2
Anti-Pfaffian	1/2	1	non-univ.	1

ACKNOWLEDGMENTS

It is a pleasure to thank Moty Heiblum and Bivas Dutta for illuminating discussions on this topic. This work was partially supported through CRC/Transregio 183, by the ERC (LEGOTOP), the ISF (1866/17) and within the ISF-Quantum program.

- ¹ D. C. Tsui, H. L. Stormer, and A. C. Gossard, “Two-dimensional magnetotransport in the extreme quantum limit,” *Phys. Rev. Lett.* **48**, 1559 (1982).
- ² R. B. Laughlin, “Anomalous quantum Hall effect: An incompressible quantum fluid with fractionally charged excitations,” *Phys. Rev. Lett.* **50**, 1395 (1983).
- ³ F. D. M. Haldane, “Fractional quantization of the Hall effect: A hierarchy of incompressible quantum fluid states,” *Phys. Rev. Lett.* **51**, 605 (1983).
- ⁴ R. Rammal, G. Toulouse, M. T. Jaekel, and B. I. Halperin, “Quantized Hall conductance and edge states: Two-dimensional strips with a periodic potential,” *Phys. Rev. B* **27**, 5142 (1983).
- ⁵ B. I. Halperin and J. K. Jain, *Fractional Quantum Hall Effects* (WORLD SCIENTIFIC, 2020) <https://www.worldscientific.com/doi/pdf/10.1142/11751>.
- ⁶ X. G. Wen, “Non-Abelian statistics in the fractional quantum Hall states,” *Phys. Rev. Lett.* **66**, 802–805 (1991).
- ⁷ C. Nayak, S. H. Simon, A. Stern, M. Freedman, and S. Das Sarma, “Non-Abelian anyons and topological quantum computation,” *Rev. Mod. Phys.* **80**, 1083 (2008).
- ⁸ G. Moore and N. Read, “Nonabelions in the fractional quantum Hall effect,” *Nucl. Phys. B* **360**, 362 (1991).
- ⁹ N. Read and D. Green, “Paired states of fermions in two dimensions with breaking of parity and time-reversal symmetries and the fractional quantum Hall effect,” *Phys. Rev. B* **61**, 10267 (2000).
- ¹⁰ R. H. Morf, “Transition from quantum Hall to compressible states in the second Landau level: New light on the $\nu = 5/2$ enigma,” *Phys. Rev. Lett.* **80**, 1505 (1998).
- ¹¹ E. H. Rezayi and F. D. M. Haldane, “Incompressible paired Hall state, stripe order, and the composite fermion liquid phase in half-filled Landau levels,” *Phys. Rev. Lett.* **84**, 4685 (2000).
- ¹² M. R. Peterson, Th. Jolicoeur, and S. Das Sarma, “Finite-layer thickness stabilizes the Pfaffian state for the $5/2$ fractional quantum Hall effect: Wave function overlap and topological degeneracy,” *Phys. Rev. Lett.* **101**, 016807 (2008).
- ¹³ A. Wójs, C. Toke, and J. K. Jain, “Landau-level mixing and the emergence of Pfaffian excitations for the $5/2$ fractional quantum Hall effect,” *Phys. Rev. Lett.* **105**, 096802 (2010).
- ¹⁴ M. Storni, R. H. Morf, and S. Das Sarma, “Fractional quantum Hall state at $\nu = 5/2$ and the Moore-Read Pfaffian,” *Phys. Rev. Lett.* **104**, 076803 (2010).
- ¹⁵ E. H. Rezayi and S. H. Simon, “Breaking of particle-hole symmetry by Landau level mixing in the $\nu = 5/2$ quantized Hall state,” *Phys. Rev. Lett.* **106**, 116801 (2011).
- ¹⁶ A. E. Feiguin, E. Rezayi, C. Nayak, and S. Das Sarma, “Density matrix renormalization group study of incompressible fractional quantum Hall states,” *Phys. Rev. Lett.* **100**, 166803 (2008).
- ¹⁷ A. E. Feiguin, E. Rezayi, K. Yang, C. Nayak, and S. Das Sarma, “Spin polarization of the $\nu = 5/2$ quantum Hall state,” *Phys. Rev. B* **79**, 115322 (2009).
- ¹⁸ M. Levin, B. I. Halperin, and B. Rosenow, “Particle-hole symmetry and the Pfaffian state,” *Phys. Rev. Lett.* **99**, 236806 (2007).
- ¹⁹ S. S. Lee, S. Ryu, C. Nayak, and M. P. A. Fisher, “Particle-hole symmetry and the $\nu = 5/2$ quantum Hall state,” *Phys. Rev. Lett.* **99**, 236807 (2007).
- ²⁰ R. Willett, “The quantum Hall effect at $5/2$ filling factor,” *Reports on Progress in Physics* **76**, 076501 (2013).
- ²¹ A. Stern and B. I. Halperin, “Proposed experiments to probe the non-Abelian $\nu = 5/2$ quantum Hall state,” *Phys. Rev. Lett.* **96**, 016802 (2006).
- ²² P. Bonderson, A. Kitaev, and K. Shtengel, “Detecting non-Abelian statistics in the $\nu = 5/2$ fractional quantum Hall state,” *Phys. Rev. Lett.* **96**, 016803 (2006).
- ²³ M. Banerjee, M. Heiblum, V. Umansky, D. E. Feldman, Y. Oreg, and A. Stern, “Observation of half-integer thermal Hall conductance,” *Nature* **559**, 205 (2018).
- ²⁴ D. T. Son, “Is the composite Fermion a Dirac particle?” *Phys. Rev. X* **5**, 031027 (2015).
- ²⁵ The generic state in this phase does not need to be PH-symmetric,⁵³ but will map onto different state in the same phase.
- ²⁶ L. Antonic, J. Vucicevic, and M. V. Milovanovic, “Paired states at $5/2$: Particle-hole Pfaffian and particle-hole symmetry breaking,” *Phys. Rev. B* **98**, 115107 (2018).
- ²⁷ M. V. Durdevic, S. and Milovanovic, “Model interactions for Pfaffian paired states based on Chern-Simons field theory description,” *Phys. Rev. B* **100**, 195303 (2019).
- ²⁸ A. C. Balram, M. Barkeshli, and M. S. Rudner, “Parton construction of a wave function in the anti-Pfaffian phase,” *Phys. Rev. B* **98**, 035127 (2018).
- ²⁹ R. V. Mishmash, D. F. Mross, J. Alicea, and O. I. Motrunich, “Numerical exploration of trial wave functions for the particle-hole-symmetric Pfaffian,” *Phys. Rev. B* **98**, 081107 (2018).
- ³⁰ M. Yutushui and D. F. Mross, “Large-scale simulations of particle-hole-symmetric Pfaffian trial wave functions,” *Phys. Rev. B* **102**, 195153 (2020).
- ³¹ E. H. Rezayi, K. Pakrouski, and F. D. M. Haldane, “Energetics of the PH-Pfaffian state and the $5/2$ -fractional quantum Hall effect,” (2021), [arXiv:2103.12026 \[cond-mat.mes-hall\]](https://arxiv.org/abs/2103.12026).
- ³² S. H. Simon, “Interpretation of thermal conductance of the $\nu = 5/2$ edge,” *Phys. Rev. B* **97**, 121406(R) (2018).
- ³³ D. E. Feldman, “Comment on ‘interpretation of thermal conductance of the $\nu = 5/2$ edge’,” *Phys. Rev. B* **98**, 167401 (2018).
- ³⁴ S. H. Simon, “Reply to ‘comment on ‘interpretation of thermal conductance of the $\nu = 5/2$ edge’ ’,” *Phys. Rev. B* **98**, 167402 (2018).
- ³⁵ Ken K. W. Ma and D. E. Feldman, “Partial equilibration of integer and fractional edge channels in the thermal quantum Hall effect,” *Phys. Rev. B* **99**, 085309 (2019).
- ³⁶ S. H. Simon and B. Rosenow, “Partial equilibration of the anti-Pfaffian edge due to Majorana disorder,” *Phys. Rev. Lett.* **124**, 126801 (2020).
- ³⁷ Hamed Asasi and Michael Mulligan, “Partial equilibration of anti-Pfaffian edge modes at $\nu = 5/2$,” *Phys. Rev. B* **102**, 205104 (2020).
- ³⁸ B. Dutta, W. Yang, R. A. Melcer, H. K. Kundu, M. Heiblum, V. Umansky, Y. Oreg, A. Stern, and D. Mross, “Novel method distinguishing between competing topological orders,” (2021), [arXiv:2101.01419 \[cond-mat.mes-hall\]](https://arxiv.org/abs/2101.01419).
- ³⁹ Implication of these terms for thermal equilibration are discussed in Ref. 54.

- ⁴⁰ C. L. Kane, M. P. A. Fisher, and J. Polchinski, “Randomness at the edge: Theory of quantum Hall transport at filling $\nu=2/3$,” *Phys. Rev. Lett.* **72**, 4129–4132 (1994).
- ⁴¹ C. L. Kane and M. P. A. Fisher, “Impurity scattering and transport of fractional quantum Hall edge states,” *Phys. Rev. B* **51**, 13449–13466 (1995).
- ⁴² J. E. Moore and X. G. Wen, “Classification of disordered phases of quantum Hall edge states,” *Phys. Rev. B* **57**, 10138–10156 (1998).
- ⁴³ J. E. Moore and X. G. Wen, “Critical points in edge tunneling between generic fractional quantum Hall states,” *Phys. Rev. B* **66**, 115305 (2002).
- ⁴⁴ D. Ferraro, A. Braggio, N. Magnoli, and M. Sasseti, “Charge tunneling in fractional edge channels,” *Phys. Rev. B* **82**, 085323 (2010).
- ⁴⁵ I.V. Protopopov, Yuval Gefen, and A.D. Mirlin, “Transport in a disordered $\nu = 2/3$ fractional quantum Hall junction,” *Annals of Physics* **385**, 287 – 327 (2017).
- ⁴⁶ T. Giamarchi and H. J. Schulz, “Anderson localization and interactions in one-dimensional metals,” *Phys. Rev. B* **37**, 325–340 (1988).
- ⁴⁷ S. B. Chung, X. L. Qi, J. Maciejko, and S. C. Zhang, “Conductance and noise signatures of majorana backscattering,” *Phys. Rev. B* **83**, 100512 (2011).
- ⁴⁸ D. L. Maslov and M. Stone, “Landauer conductance of Luttinger liquids with leads,” *Phys. Rev. B* **52**, R5539–R5542 (1995).
- ⁴⁹ I. Safi and H. J. Schulz, “Transport in an inhomogeneous interacting one-dimensional system,” *Phys. Rev. B* **52**, R17040–R17043 (1995).
- ⁵⁰ V. V. Ponomarenko, “Renormalization of the one-dimensional conductance in the Luttinger-liquid model,” *Phys. Rev. B* **52**, R8666–R8667 (1995).
- ⁵¹ B. Rosenow and B. I. Halperin, “Signatures of neutral quantum Hall modes in transport through low-density constrictions,” *Phys. Rev. B* **81**, 165313 (2010).
- ⁵² H. H. Lai and K. Yang, “Distinguishing particle-hole conjugated fractional quantum Hall states using quantum-dot-mediated edge transport,” *Phys. Rev. B* **87**, 125130 (2013).
- ⁵³ P. T. Zucker and D. E. Feldman, “Stabilization of the particle-hole Pfaffian order by Landau-level mixing and impurities that break particle-hole symmetry,” *Phys. Rev. Lett.* **117**, 096802 (2016).
- ⁵⁴ Ken K. W. Ma and D. E. Feldman, “Thermal equilibration on the edges of topological liquids,” *Phys. Rev. Lett.* **125**, 016801 (2020).

Appendix A: Conductance of particle-hole conjugate setup

We now compute the conductance between the source S and the drain D1 for the setup in Fig. 1(b) (see also Refs. 48–50). We begin with the case of density-density interactions but no tunneling. The edge theory is then governed by the action

$$S_0 = \frac{1}{4\pi} \int d\tau dx \begin{pmatrix} \partial_x \phi & \partial_x \varphi \end{pmatrix} \begin{pmatrix} -i\partial_\tau + v\partial_x & -h\partial_x \\ -h\partial_x & 2(i\partial_\tau + v\partial_x) \end{pmatrix} \begin{pmatrix} \phi \\ \varphi \end{pmatrix}. \quad (\text{A1})$$

The eigenmodes ϕ_R, ϕ_L of the composite edge are related to the underlying electron ϕ and semion φ modes via $(\phi_R, \phi_L) = \hat{W}(\phi, \sqrt{2}\varphi)$, where

$$\hat{W} = \begin{pmatrix} \sqrt{1+b^2} & b \\ b & \sqrt{1+b^2} \end{pmatrix}, \quad b = \frac{1}{\sqrt{2}} \left(\frac{1}{\sqrt{1-2h^2/(v_e+v)^2}} - 1 \right)^{\frac{1}{2}}. \quad (\text{A2})$$

The absence of tunneling demands conservation of semion and electron currents separately at each junction, i.e., $I_e^S = I_e^{D2}$, $I_e^{D1} = I_e^{D3}$ and $I_{qp} = I_{qp}^{D2} = I_{qp}^{D3}$. Furthermore, the drains D2 and D3 do not inject currents and thus $I_L^{D2} = 0$ and $I_R^{D3} = 0$. From these conditions, we determine the semion current in the middle region I_{qp} and the electron current flowing into the drain D1

$$I_{qp} = I_e^S \frac{b}{\sqrt{2(1+b^2)}}, \quad I_e^{D1} = I_{qp} \frac{\sqrt{2}b}{\sqrt{1+b^2}}. \quad (\text{A3})$$

Thus, the conductance between the source and the drain D1 is given by $G = \frac{b^2}{b^2+1}$. For a non-interacting edge $h = 0$, all of the current flows into D2 yielding the conductance $G = 0$.

The conductance becomes universal when random tunneling along the arms leading to D2, D3 is included [see in Fig. 1(c) and 2(c)]. As we explained above app. B, this type of disorder can be gauged out for the half-infinite wire, e.g., the leads at D2 and D3. Nevertheless, it still renormalizes the density-density interactions h to its fixed value $h_* = \frac{2}{3}(v_e + v)$. According to Eq. (A2), this amounts to $b = 1$ and thus $G = 1/2$.

Appendix B: Disordered fixed points of the anti-Pfaffian edge

We now employ the methods of Ref. 18 and 19 to analyze the disordered fixed point of a finite anti-Pfaffian edge. Our analysis parallels the one performed in Refs. 45 for the $\nu = 2/3$ edge. We use the setup of Fig. 2(a), where the

anti-Pfaffian edge is the one occurring between $\nu = 3$ and the Moore-Read state. In the outer regions $x < x_L$ and $x > x_R$, electron ϕ , semion φ and Majorana γ modes are decoupled, while in the middle region $x \in [x_L, x_R]$ the two edges are close to one another, such that tunneling and interactions are allowed. They are described by

$$\mathcal{L}_{\text{tun}} = i\lambda(x)\gamma e^{i\phi-2i\varphi} + \text{H.c.}, \quad \mathcal{L}_{\text{int}} = 2h\partial_x\phi\partial_x\varphi. \quad (\text{B1})$$

As in the main text, we define charge $\varphi_c = \phi - \varphi$ and neutral $\phi_n = \phi - 2\varphi$ modes. When the disorder is relevant, i.e., for $h_{\text{bare}} > h_c$ the middle region flows towards the anti-Pfaffian fixed point, where φ_c and ϕ_n modes are decoupled ($h = h_*$), and the ϕ_n and Majorana modes have the same velocity v . We now define a three-component real fermion, $\Psi = (\text{Re}[e^{i\phi_n}], \text{Im}[e^{i\phi_n}], \gamma)$. The disordered tunneling term can be written in terms of this fermion as $\mathcal{L}_{\text{tun}} \propto i\Psi^T \hat{\lambda} \Psi$, where $\hat{\lambda} = \text{Im}[\lambda]\hat{L}_x + \text{Re}[\lambda]\hat{L}_y$ and \hat{L}_i are generators of $SO(3)$. Then, the problem is greatly simplified by constructing $SO(3)$ -rotation $\tilde{\Psi}(x) = \hat{U}(x)\Psi(x)$ such that:

- $\hat{U}(x)$ does not change the Hamiltonian in the outer regions.
- $\hat{U}(x)$ eliminates the tunneling in the middle region.
- $\hat{U}(x)$ is continuous everywhere, but a single point, for definiteness at $x = x_R$.

Similarly to Ref. 45, such a rotation can be constructed as

$$\hat{U}(x) = \begin{cases} R_z(\alpha), & x < x_L \\ R_z(\alpha)\mathcal{P} \exp\left[\frac{1}{v} \int_{x_L}^x \hat{\lambda}(x')dx'\right], & x \in [x_L, x_R] \\ R_z(\beta), & x > x_R \end{cases} \quad (\text{B2})$$

where \mathcal{P} is a path-ordering, $R_z(\alpha)$ and $R_z(\beta)$ are rotations around z -axis defined by the Euler decomposition

$$\mathcal{P} \exp\left[\frac{1}{v} \int_{x_L}^{x_R} \hat{\lambda}(x')dx'\right] \equiv R_z^{-1}(\alpha)R_x(\theta)R_z(\beta). \quad (\text{B3})$$

In the outer regions, $\hat{U}(x)$ preserves $\Psi_z = \gamma$ and $\partial_x\phi_n \propto \psi_n^\dagger\psi_n \propto \Psi^T \hat{L}_z \Psi$, the only terms that appear in the Lagrangian density there. In the middle region, the λ -dependent rotation absorbs \mathcal{L}_{tun} into the kinetic term, at the price of introducing the complicated boundary conditions $\tilde{\Psi}(x_R^-) = R_x(\theta)\tilde{\Psi}(x_R^+)$, where $x_R^\pm \equiv \lim_{\epsilon \rightarrow 0} x_R \pm \epsilon$. Generically, these boundary conditions mix γ and $e^{i\phi_n}$. They greatly simplify for the specific values of θ equal to 0 or π , which we denote θ_* . Here the discontinuity reads as $\tilde{\phi}_n(x_R^\pm) = \pm\phi_n(x_R)$ and $\tilde{\gamma}(x_R^\pm) = \pm\gamma(x_R)$. For these configurations, the theory is Gaussian, and thus describes a fixed point.

Consider now a small deviation from these fixed points, i.e., $\theta = \theta_* + \delta\theta$. Instead of working with complicated boundary conditions that mix γ and $e^{i\phi_n}$, it is convenient to perform an incomplete gauge transformation \hat{U}_{θ_*} similar to Eq. (B2) but with different $\hat{\Lambda}(x)$ (see also Ref. 45). We define $\hat{\Lambda}(x)$ such that it is equal to $\hat{\lambda}(x)$ everywhere except a small vicinity of $x = x_0 \in [x_L, x_R]$. The profile of $\hat{\Lambda}$ around x_0 has to be chosen such that the Euler decomposition Eq. (B3) of $\hat{U}_{\theta_*}(x)$ gives θ_* instead of θ (with possibly different α and β). The price for having simple boundary conditions is a residual term left at a single point x_0 when the vicinity has shrunk to a point

$$\delta\mathcal{L}_{\text{tun}} \propto iv\delta\theta\tilde{\gamma} \sin(\tilde{\phi}_n)\delta(x - x_0). \quad (\text{B4})$$

The relevance of this perturbation determines the stability of the fixed point. Notice that the discontinuity and the residual tunneling may be independently chosen to be anywhere in $[x_L, x_R]$. We choose the former to be at x_R and the latter at $x_0 \in (x_L, x_R)$.

1. Stability of the fixed points

Now, we study the RG flow of the remaining tunneling term Eq. (B4). Since it only operates at a single point, we have

$$\frac{d\delta\theta}{d\log[\Lambda_\omega]} = [1 - \Delta_\gamma^{\theta_*}(\Lambda_\omega) - \Delta_{\psi_n}^{\theta_*}(\Lambda_\omega)]\delta\theta, \quad (\text{B5})$$

where Λ_ω is a frequency cut-off. $\Delta_\gamma^{\theta_*}(\Lambda_\omega), \Delta_{\psi_n}^{\theta_*}(\Lambda_\omega)$ are the scaling dimensions of the Majorana fermion γ and the neutral fermion ψ_n , respectively. The former is given by $\Delta_\gamma = 1/2$ at either fixed point. It remains to determine Δ_{ψ_n} , which is encoded in the Green function $D_n(\omega) \equiv \langle \phi_n(-\omega, x_0) \phi_n(\omega, x_0) \rangle$, evaluated at $\delta_\theta = 0$.

Precisely at the fixed point, the bosonic modes ϕ, φ that comprise ϕ_n decouple from the Majorana. They are described by the Lagrangian density

$$\mathcal{L}_0 = \frac{1}{4\pi} \begin{pmatrix} \partial_x \phi & \partial_x \varphi \end{pmatrix} \begin{pmatrix} -i\partial_\tau + v_\phi(x)\partial_x & -h(x)\partial_x \\ -h(x)\partial_x & 2(i\partial_\tau + v_\varphi(x)\partial_x) \end{pmatrix} \begin{pmatrix} \phi \\ \varphi \end{pmatrix} \quad (\text{B6})$$

where the density-density interaction vanishes unless $x \in [x_L, x_R]$. There, it is renormalized to the value h_* as specified in the main text. We compute $D_n(\omega)$ for the special case $v_\phi(x) = v_\varphi(x) = v$ where the algebra simplifies considerably. We introduce the pair of canonical bosons $\Theta = \frac{\phi + \sqrt{2}\varphi}{2}$ and $\Phi = \frac{\phi - \sqrt{2}\varphi}{2}$ to bring \mathcal{L}_0 to a familiar form, i.e.,

$$\mathcal{L}_0 = \frac{i}{\pi} \partial_x \Theta \partial_\tau \Phi + \frac{1}{2\pi} \frac{u(x)}{K(x)} [\partial_x \Theta]^2 + \frac{u(x)K(x)}{2\pi} [\partial_x \Phi]^2. \quad (\text{B7})$$

Along the composite edge, $x \in [x_L, x_R]$, the parameters are $u(x) = \frac{v}{3}$ and $K(x) = K_* = \frac{\sqrt{2}-1}{\sqrt{2}+1}$, outside they are given by $u(x) = v$ and $K(x) = 1$. The neutral field in this basis becomes $\phi_n = (\sqrt{2}+1)\Theta + (\sqrt{2}-1)\Phi$. The correlation functions that contribute to the scaling dimension of ψ_n are $D_\Theta(\omega) \equiv \langle \Theta(-\omega, x_0) \Theta(\omega, x_0) \rangle$ and $D_\Phi(\omega) \equiv \langle \Phi(-\omega, x_0) \Phi(\omega, x_0) \rangle$. They can be separately computed by integrating Φ and Θ correspondingly.

Trivial fixed point. Near the trivial fixed point $\theta_* = 0$, the Green's functions can be easily computed in complete analogy with Ref. 48

$$D_\Theta^0(\omega) = \frac{K_*}{2|\omega|} \frac{\left(1 + \sqrt{2}e^{\frac{\omega L}{u(x_0)}}\right)^2 + 4\sqrt{2}e^{\frac{\omega L}{u(x_0)}} \sinh\left[\frac{\omega x_0}{u(x_0)}\right]^2}{\left(1 - 2e^{\frac{2\omega L}{u(x_0)}}\right)}, \quad (\text{B8})$$

$$D_\Phi^0(\omega) = \frac{1}{2|\omega|K_*} \frac{\left(1 - \sqrt{2}e^{\frac{\omega L}{u(x_0)}}\right)^2 - 4\sqrt{2}e^{\frac{\omega L}{u(x_0)}} \sinh\left[\frac{\omega x_0}{u(x_0)}\right]^2}{\left(1 - 2e^{\frac{2\omega L}{u(x_0)}}\right)}, \quad (\text{B9})$$

where without loss of generality, we set $x_{R,L} = \pm \frac{L}{2}$. We find that the effective ω -dependent scaling dimension of ψ_n does not depend on x_0 and is given by

$$\Delta_{\psi_n}^0(\omega) = -|\omega| \frac{D_\Theta(\omega)(\sqrt{2}+1)^2 + D_\Phi(\omega)(\sqrt{2}-1)^2}{2} = \frac{1}{2} \left(\frac{2e^{\frac{2\omega L}{u(x_0)}} + 1}{2e^{\frac{2\omega L}{u(x_0)}} - 1} \right). \quad (\text{B10})$$

It takes the free-fermion value $1/2$ for $\omega \rightarrow \infty$; it grows with decreasing frequency and has the asymptotic value $\Delta_{\psi_n}^0(\omega = 0) = \frac{3}{2}$. The tunneling term is thus an irrelevant perturbation at the trivial fixed point.

Twisted fixed point. At the twisted fixed point $\theta_* = \pi$, thus the neutral field ϕ_n changes sign across x_R , corresponding to the boundary conditions $\Theta(x_R^-) = K_*\Phi(x_R^+)$ and $\Phi(x_R^-) = K_*^{-1}\Theta(x_R^+)$. We thus define new continuous fields $\tilde{\Theta}, \tilde{\Phi}$ which coincide with Θ, Φ at $x < x_R$ and satisfy $\tilde{\Theta} = K_*\Phi$ and $\tilde{\Phi} = K_*^{-1}\Theta$ for $x > x_R$. In term of these fields, the action looks the same as Eq. (B7) with the same velocity profile and a new Luttinger parameter that takes the values $K(x < x_L) = 1, K(x_L < x < x_R) = K_*$ and $K(x > x_R) = K_*^2$. The corresponding Green's functions are

$$D_{\tilde{\Theta}}^\pi(\omega) = \frac{K_*}{2|\omega|} \frac{1 - 2e^{\frac{2\omega L}{u(x_0)}} + 2\sqrt{2}e^{\frac{\omega L}{u(x_0)}} \sinh\left[\frac{2\omega x_0}{u(x_0)}\right]}{1 + 2e^{\frac{2\omega L}{u(x_0)}}}, \quad (\text{B11})$$

$$D_{\tilde{\Phi}}^\pi(\omega) = \frac{1}{2|\omega|K_*} \frac{1 - 2e^{\frac{2\omega L}{u(x_0)}} - 2\sqrt{2}e^{\frac{\omega L}{u(x_0)}} \sinh\left[\frac{2\omega x_0}{u(x_0)}\right]}{1 + 2e^{\frac{2\omega L}{u(x_0)}}}. \quad (\text{B12})$$

Thus, the effective scaling dimension of ψ_n at the twisted fixed point is

$$\Delta_{\psi_n}^\pi(\omega) = \frac{1}{2} \left(\frac{2e^{\frac{2\omega L}{u(x_0)}} - 1}{2e^{\frac{2\omega L}{u(x_0)}} + 1} \right). \quad (\text{B13})$$

For large frequencies $\omega \gg u(x_0)/L$ the effective scaling dimensions of ψ_n at the two fixed points coincide. In this limit, the Green's functions are dominated by short distances $\lesssim u(x_0)/\omega$ around x_0 and thus become insensitive to the boundary condition at x_R . By contrast, in the low-frequency limit, the effective scaling dimension becomes $\Delta_{\psi_n}^\pi(0) = \frac{1}{6}$, while $\Delta_{\psi_n}^0(0) = \frac{3}{2}$. The tunneling is thus relevant at the twisted fixed point.

Other fillings. The result obtained here can be extended to other filling factors such as $\nu = 2/3$, where the system's fate is determined by the scaling dimension of the tunneling of an electron between the integer and fractional $\nu = 1/3$ modes. For generality, we provide an expression for the scaling dimension of the tunneling operator $e^{i(\phi-n\varphi)}$ for a composite edge with an integer mode ϕ and a fractional $\nu = \frac{1}{n}$ mode φ described by an action analogous to Eq. (B6). Taking the interaction in the region between x_L and x_R to be $h_* = \frac{2n\nu}{n+1}$ such that charge and neutral modes decouple there, we find

$$\Delta_0(\omega) = \frac{n-1}{2} \left(\frac{ne^{\frac{2\omega L}{u(x_0)} + 1}}{\frac{2\omega L}{u(x_0)} - 1} \right), \quad \Delta_\pi(\omega) = \frac{n-1}{2} \left(\frac{ne^{\frac{2\omega L}{u(x_0)} - 1}}{\frac{2\omega L}{u(x_0)} + 1} \right), \quad (\text{B14})$$

where $u(x_0) = \frac{n-1}{n+1}v$. For the $\nu = 2/3$ case, Eqs. (B14) matches the integral forms of the same quantities derived in Ref. 45.

2. Conductance at the fixed points

Utilizing Kubo formalism for chiral wires (see, e.g. Ref. 51), we compute the conductance between the source S and the drain D1 as a retarded correlation function of electron currents at $x < x_L$ and $x' > x_R$

$$G = - \lim_{\omega \rightarrow 0} \omega \langle \phi(-\omega, x) \phi(\omega, x') \rangle. \quad (\text{B15})$$

Conductance at the trivial fixed point. In the case of trivial fixed point, both ϕ to the left and the right of the junction are expressed as $\phi = \Phi + \Theta$. In the zero-frequency limit, the correlation function $\langle \Phi\Theta \rangle$ does not contribute to the conductance. Thus $\langle \Phi\Phi \rangle$ and $\langle \Theta\Theta \rangle$ can be computed separately

$$\lim_{\omega \rightarrow 0} \omega \langle \phi(-\omega, x) \phi(\omega, x') \rangle = \lim_{\omega \rightarrow 0} \omega [D_\Phi(\omega, x, x') + D_\Theta(\omega, x, x')]. \quad (\text{B16})$$

For the trivial fixed point, at small frequencies $D_\Phi(\omega, x, x') = D_\Theta(\omega, x, x') = \frac{1}{2|\omega|}$, and the expected result of unit conductance is obtained.⁴⁸⁻⁵⁰

Conductance at the twisted fixed point. At the twisted fixed point, the field ϕ to the right of the junction is expressed as $\phi = K_*\tilde{\Phi} + K_*^{-1}\tilde{\Theta}$, while to the left of the junction, it is not modified. Thus, the conductance becomes

$$\lim_{\omega \rightarrow 0} \omega \langle \phi(-\omega, x) \phi(\omega, x') \rangle = \lim_{\omega \rightarrow 0} \omega [K_*D_{\tilde{\Phi}}(\omega, x, x') + K_*^{-1}D_{\tilde{\Theta}}(\omega, x, x')]. \quad (\text{B17})$$

Using the effective Luttinger parameters for the three regions, we compute $D_{\tilde{\Phi}}, D_{\tilde{\Theta}}$ separately and find the conductance $G = \frac{n-1}{n+1}$. This value agrees with the simple current calculation Eq. (4) and the result found in Ref. 45 for the $\nu = \frac{2}{3}$ edge.